引用格式：QI Tiantian, LIU Wei, THOMAS J C, et al. Determination of Optimal Autocorrelation Function Truncation Point for Particle Size Measurement with Dynamic Light Scattering[J]. Acta Photonica Sinica, 2022, 51(3):0329001
齐甜甜,刘伟,THOMAS J C,等.动态光散射颗粒测量中相关函数最优截断点的确定[J].光子学报,2022,51(3):0329001

动态光散射颗粒测量中相关函数最优截断点的确定

齐甜甜[1],刘伟[1],THOMAS J C[1,2],贾宏燕[1],魏芹芹[1],王雅静[1],申晋[1]
(1 山东理工大学 电气与电子工程学院,山东 淄博 255049)
(2 科学集团有限公司,澳大利亚 南澳大利亚州 葛兰许 5022)

摘 要:从动态光散射信号中反演纳米颗粒粒度分布,结果准确性和重复性受测量的自相关函数数据点影响,数据点长度不同会导致不同的反演结果。为了解决该问题,提出了一种根据拟合自相关函数的均方根误差来截断自相函数的方法,该方法通过设置拟合误差阈值来自适应地选择最佳自相关函数数据点数。实验结果表明,使用均方根误差阈值方法获得的颗粒粒度分布比其他方法获得的结果具有更高的准确性和更好的重复性。

关键词:动态光散射;光子相关光谱;最佳数据点;自相关函数;均方根误差;颗粒粒度分布;纳米颗粒测量

中图分类号:O439 **文献标识码**:A **doi**:10.3788/gzxb20225103.0329001

0 Introduction

Dynamic Light Scattering (DLS) also known as photon correlation spectroscopy, is a common method for the determination of particle size in nano-particle suspensions[1-2]. Determination of the particle size distribution (PSD) from the measured intensity Autocorrelation Function (ACF) is an ill-posed inversion problem involving a Fredholm integral equation of the first kind. This is a notorious problem in which small variations in the ACF data can result in large changes in the recovered PSD. A variety of algorithms have been proposed for solving this inversion problem [3-9]. Both the simulated and measured results showed that, if all ACF points were used in the inversion, the PSD results were less accurate, due to the larger noise of the ACF data as it approached the baseline.

RUF H[10] examined the effect of normalization error on the PSD obtained from DLS data and concluded that a more accurate PSD is obtained if the number of ACF points is properly reduced, and when the first 70 points are used only, the original distribution is retrieved. RUF H and GOULD B J[11] found that omitting the last 46 points of the ACF gave the best results for the PSD of chylomicrons from human lymph. RUF H[12] looked at the effect of nonrandom errors on the results of regular inversion of DLS data and proposed that the value of ACF down to 0.001 can be used in the inversion. CLEMENTI L A[13] proposed a Bayesian inversion method for estimating the PSD of latexes from multiangle DLS. They limited the ACF to its first 30 points to ensure an acceptable signal-to-noise ratio. YUAN Xi[9] investigated the effect of the number of ACF data points and the PSD fraction on the recovered PSD results and concluded that the optimal number of PSD

Foundation item: Key Research and Development Project of Guangdong Province(No.2020B0101320002), Natural Science Foundation of Shandong Province(No.ZR2020MF124), Key Research and Development Program of Shandong Province (No.2019GGX104017)
First author: QI Tiantian (1993—), female, M. D. candidate, mainly focuses on dynamic light scattering measurement. Email: 1655542554@qq.com
Supervisor(**Contact author**): LIU Wei(1971—), male, professor, Ph. D., mainly focuses on particle measurement technology. Email: weikey@sdut.edu.cn
Received: Jul.7,2021; **Accepted**: Sep.6,2021

sampling points is limited by the ACF points used in the analysis, but the article did not mention how to select ACF points. In current practice, a fixed number of ACF points or a fixed ACF threshold is usually used to select the number of ACF points to recover the PSD. The selection of the optimal ACF data points is not only related to the size of the measured particles, but also to the accuracy of the measured ACF, the appropriate number of ACF data points helps to improve the accuracy of the inversion results.However, neither of these two methods can take account of the measured particle size and the accuracy of the measured ACF.

In response to this problem, we propose a root-mean-square error threshold method based on that the noise in the long delay part of the ACF is larger than that in the short delay part and that the root-mean-square error of the fitted ACF has a characteristic variation with the number of ACF data points being fitted. This novel method has strong adaptability that can adaptively select the optimal number of ACF points according to the measured particle size and the accuracy of the measured ACF. This method could improve the accuracy and repeatability of the recovered results, and has high practical significance and value.

1 Basic principles

Assuming the scattered light field satisfies the Gaussian statistical, the intensity ACF $g^{(2)}(\tau)$ is related to the electric field ACF $g^{(1)}(\tau)$ by the Siegert relationship [1,14]

$$g^{(2)}(\tau)=1+\beta\left|g^{(1)}(\tau)\right|^2 \tag{1}$$

where β is the optical coherence factor and t is the delay time. According to Eq. (2), the PSD $f(D)$ is obtained by inversion of

$$g^{(1)}(\tau_j)=\sum_{i=1}^{n}\exp(-k\tau_j/D_i)f(D_i)\quad j=1,2,3,\cdots,m\ ;\ i=1,2,3,\cdots,n \tag{2}$$

here j is the number of correlator channels, i.e. the number of ACF points; i is the number of points on the PSD size fraction (in this paper the total fraction number is set to 100); and $\exp(-k\tau/D)$ is the kernel function that converts from $g^{(1)}(\tau)$ to $f(D)$, in which $k=\left(k_{\mathrm{B}}T/3\pi\eta\right)\left(4\pi n\sin(\theta/2)/\lambda_0\right)^2$, k_{B} is the Boltzman constant, T is the absolute temperature, η is the viscosity coefficient of the solution, n is the refractive index of the solution, θ is the scattering angle, and λ_0 is the wavelength of laser in vacuum.

Writing Eq.(2) into matrix form gives

$$\min f(x)=\left\{\|Ax-b\|_2^2\right\} \tag{3}$$

here A is the kernel function, b is the measured data $g^{(1)}(\tau)$, and x is the wanted PSD $f(D)$, which is also the least-square solution of Eq.(2).The equation is an ill-posed equation whose solution is particularly sensitive to the fluctuation of the measured data.

Tikhonov proposed a regularization method with additional constraints in the least-squares problem to solve the above ill-posed equation [7]

$$\min f(x)=\left\{\|Ax-b\|_2^2+\alpha^2\|Lx\|_2^2\right\} \tag{4}$$

in Eq.(4), the first term is the norm of the residual of the correlation function, and Ax is the fitting electric field ACF. The second term is a constraint to smooth the size of the solution, in which L is a regularization matrix and a is a regularization parameter.

2 The influence of the number of ACF data points on the inversion result

2.1 Characteristics of the ACF noise

The samples used here are polystyrene latex spheres with certified mean diameters of 33 nm±1.4 nm (Duke 3 030A), 61 nm±4 nm (Duke 3 060A), 203 nm±4 nm (Duke 3200A), 555 nm±4.5 nm (HM600) and 1 280 nm±10 nm (GBW12017). A 10 mM NaCl solution with conductivity of 1.16 mS/cm was prepared with deionized water from a UPT-I-10T ultrapure water system with 0.1 μm filters. All five samples were diluted with the NaCl solution, ultrasonicated and referred to as Samples 1~5, and sample 1 and sample 3 were combined into a mixed sample 6. A ratio sampling time correlator with 0.5 μs first channel delay time and 160

channels (data points) was used to measure these samples, and 60 data sets (ACFs) of 10 s duration were obtained for each sample.

The short delay part of the ACF curve contains a lot of information of the measured particles. As the curve decays to the baseline, there is little useful information left. Therefore, ACF data in the short delay region should be kept as much as possible. Fig.1 shows the autocorrelation function of sample 3. The blue line in the figure is the normalized intensity ACF, $g^{(2)}(\tau)$, and the red line is the electric field ACF, $g^{(1)}(\tau)$. It can be seen from Fig.1 that the noise near the ACF baseline is much larger than that in the short delay stage, especially after converting to $g^{(1)}(\tau)$, the noise is more significant.

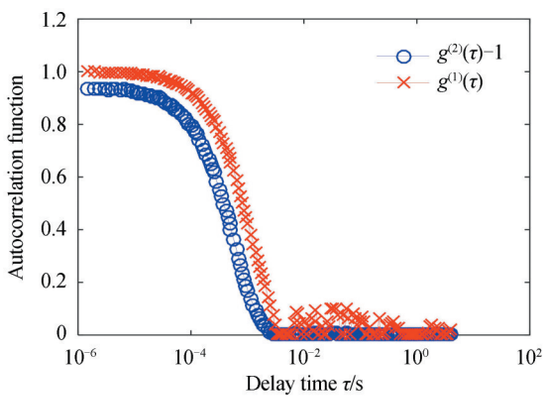

Fig.1 Normalized intensity and electric field ACF for sample 3

2.2 Root-mean-square error of fitted ACF with different data points

By inverting Eq.(4), the fitted ACF can be obtained. The deviation between the fitted ACF and the measured ACF is related to the accuracy of the recovered PSD, and it is usually measured by the fitting error of the ACF. The Root-Mean-Square Error (RMSE) is used to describe the fitting error of the ACF, as shown in Eq.(5)

$$E_{\mathrm{RMS}}=\sqrt{\frac{1}{m}\sum_{j=1}^{m}\left[\hat{g}^{(1)}(\tau_j)-g^{(1)}(\tau_j)\right]^2} \tag{5}$$

where m is the total number of ACF data points involved in the inversion, and $\hat{g}^{(1)}(\tau)=Ax$ is the fitted ACF.

Fig. 2 shows the E_{RMS} of the ACF shown in Fig. 1 as a function of the number of ACF data points used for analysis. Fig. 3 shows the fitting residual using 73 and 105 ACF data points in the analysis. It can be seen from Fig. 2 that when the number of ACF data points involved in the inversion is smaller than 73, the E_{RMS} is relatively small ($\leqslant$0.003 5) and constant. When the number of points is more than 73, the E_{RMS} increases significantly. This is related to the noise distribution in the ACF data. The measured ACF data has low noise level up to ~73 points and so the value of E_{RMS} is relatively small. There is much more noise in the data after

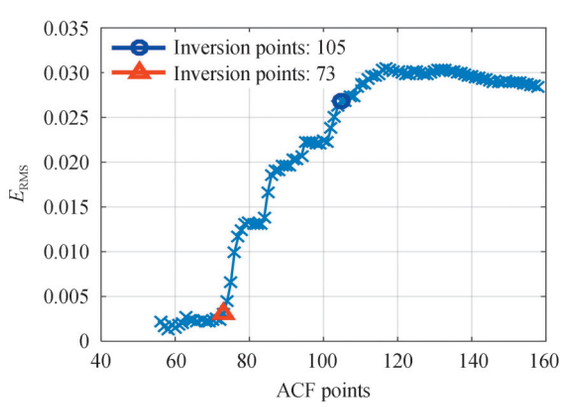

Fig.2 E_{RMS} as a function of the number of ACF data points fitted for sample 3

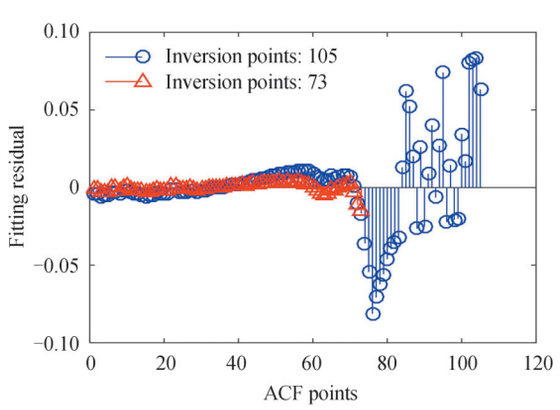

Fig.3 Fitting residuals of the ACF using 105 and 73 data points

~73 points, and the fitting error increases due to this. As shown in Fig.3, the residual values using 105 ACF data points are greater than that using 73 points. Note that the residual values at longer delay times are obviously greater than those at short delay times when 105 ACF points are used in the inversion, and this contributes to the large increase in E_{RMS}.

The distribution of noise in the ACF shown above suggests that the E_{RMS} curve as a function of number of fitted ACF points can be divided into two stages. In the first stage E_{RMS} grows smoothly and the noise level of the ACF is low; while in the second stage E_{RMS} grows rapidly, and the noise level of the ACF is high. Measurement results from samples 1, 3 and 4 at different ACF points given in Figs. 4(a), 4(b) and 4(c) show the same behaviour in E_{RMS}.

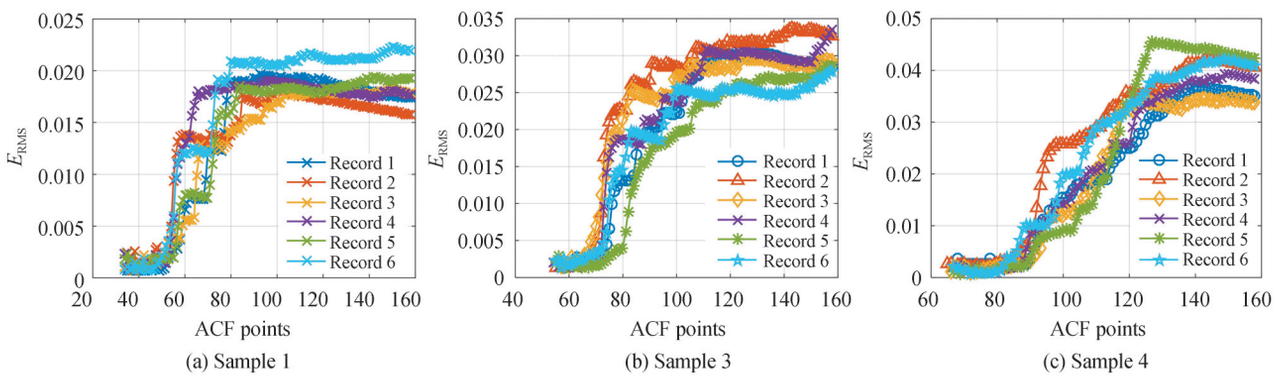

Fig.4 E_{RMS} as a function of the number of ACF data points fitted for Sample 1, Sample 3 and Sample 4

2.3 The influence of the number of ACF data points on the recovered PSD

In order to evaluate different methods, a relative error of peak position E_{PK} is defined as

$$E_{\mathrm{PK}}=\left(\frac{D_{\mathrm{peak}}-D}{D}\right)\times 100\% \tag{6}$$

here D_{peak} is the size where the peak occurs and D is the certified diameter of the samples.

The sample standard deviation of the PSD norm, S_{N}, and the sample standard deviation of the peak value, S_{D}, are defined as

$$S_{\mathrm{N}}=\sqrt{\frac{1}{N-1}\sum_{i=1}^{N}\left(N_{\mathrm{F}i}-\bar{N}_{\mathrm{F}}\right)^2} \tag{7}$$

$$S_{\mathrm{D}}=\sqrt{\frac{1}{N-1}\sum_{i=1}^{N}\left(D_{\mathrm{peak}i}-\bar{D}_{\mathrm{peak}}\right)^2} \tag{8}$$

here N is the number of measurements, $N_{\mathrm{F}i}$ is the i-th PSD norm, and $\bar{N}_{\mathrm{F}}$ is the average PSD norm; $D_{\mathrm{peak}i}$ is the i-th peak size, and $\bar{D}_{\mathrm{peak}}$ is the average peak size.

The definitions of the stability, R_{N}, and the repeatability, V_{RSD}, of the PSD are

$$R_{\mathrm{N}}=\frac{S_{\mathrm{N}}}{\bar{N}_{\mathrm{F}}}\times 100\% \tag{9}$$

$$V_{\mathrm{RSD}}=\frac{S_{\mathrm{D}}}{\bar{D}_{\mathrm{peak}}}\times 100\% \tag{10}$$

The smaller the value of R_{N}, the more stable the PSD, the smaller the value of V_{RSD}, the smaller the fluctuation of particle size, and the better the repeatability of the inversion results[15].

The long delay part of the ACF (close to the baseline) has more noise. Fig.5 and 6 respectively show the fitted ACFs and the recovered PSDs for the ACF in Fig.1 for different numbers of fitted ACF data points. Fig.7 and 8 show the stability and repeatability of 60 data sets of this sample for different numbers of ACF points being fitted, and Table 1 shows more inversion results of this sample for different numbers of ACF data points. If too many ACF points are used in the inversion, more noise is introduced, resulting in significant changes in the curvature of the fitted ACF. As shown in Fig.5, taking the fitted ACF within value between 0.96 and 0.92

as an example, there is an obvious difference among the fitted ACF for 105 points, 73 points and 59 points. It can also be seen in Fig.6 that the PSD recovered from 105 points deviates significantly from the true PSD, and false peaks are apparent. So when there are too many data points involved, the recovered peak will be inaccurate or false peaks will appear, which will cause the recovered PSD to deviate from the true PSD. It can be seen from Figs. 7 and 8 that fitting different numbers of ACF points will affect the stability and repeatability of the results.

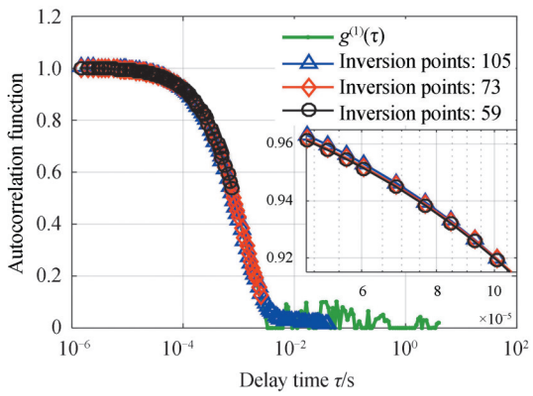

Fig.5 Fitted ACFs for sample 3 with different numbers of ACF data points being fitted

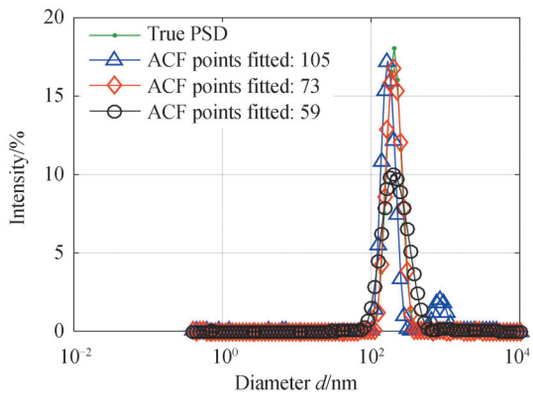

Fig.6 The PSDs of sample 3 recovered with different numbers of ACF data points being fitted

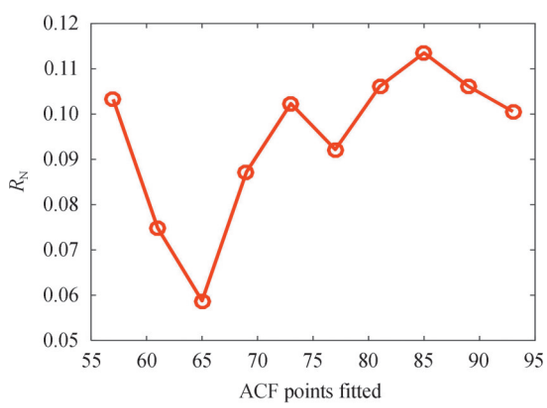

Fig.7 The R_N of sample 3 as a function of the number of ACF data points being fitted

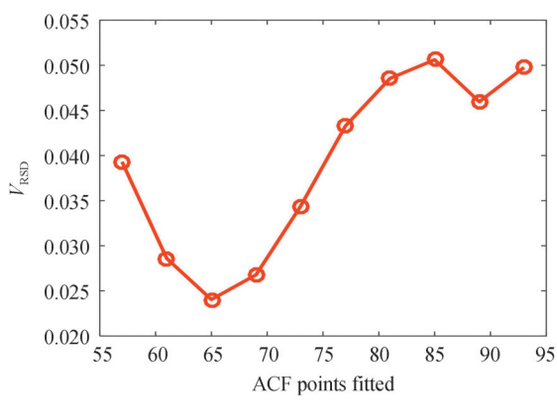

Fig.8 The V_{RSD} of sample 3 as a function of the number of ACF data points being fitted

Table 1 Inversion results of 60 data sets of Sample 3 at different numbers of ACF data points

ACF points fitted	E_{RMS}	D_{peak}/nm	E_{PK}/%	PSD width/nm	V_{RSD}/%	R_N/%
59	0.001 8	202.9	2.56	197.8	3.3	7.1
73	0.006 8	201.9	2.39	120.9	3.1	10.8
105	0.024 6	189.8	7.14	91.0	5.3	8.7

In summary, if there are too many ACF points in the inversion, the introduced noise will reduce the accuracy of the recovered PSD and false peaks may appear. On the contrary, if too few ACF points are used, sample information may be lost and the results will be inaccurate. Therefore, the key to ensuring the accuracy and stability of the results is how to choose the position to truncate the ACF, in other words, how to determine the optimal number of ACF data points to be fitted.

3 RMSE threshold method

There are two commonly used methods to select the number of ACF points to be fitted. These are

choosing a fixed number of ACF points or choosing a fixed ACF level threshold (FACFT).

For the method of a fixed number of ACF points, the same number of ACF points are used for inversion, regardless of the sample. As mentioned earlier, in order to avoid introducing noise near the ACF baseline, the number of ACF points involved in the inversion can not be too many. In this case, for small particles with fast decaying ACFs, fewer ACF points are needed for inversion, while for large particles with slow decaying ACFs, more ACF points are needed. This method can not take both large and small particles into account, so it lacks adaptability, and its inversion results are expected not be optimal.

The FACFT method first sets a specific threshold, then truncates the ACF at the position where the ACF value is less than the threshold, and this sets the number of ACF data points to be used in the inversion. It can be seen from the electric field ACF that there is a lot of noise when $g^{(1)}(\tau)<0.1$ (close to the baseline), so the empirical value of 0.1 is used as the threshold in this paper. Fig.9 shows the selection of the ACF data points by the FACFT method under different noise levels for simulated 100 nm particles. The ACF data were simulated for a log normal distribution with a peak at 100 nm and different levels of random noise was added. As shown in Fig.9, the black ○ mark is the position selected by the FACFT method. For the three noise levels of 0.01, 0.04, and 0.08, the selected ACF points are 89, 89, and 88 respectively, which are basically the same. Clearly, this method does not have the ability to respond to noise and cannot automatically adjust the optimal number of ACF points to be fitted depending on the noise level of the measured ACF data.

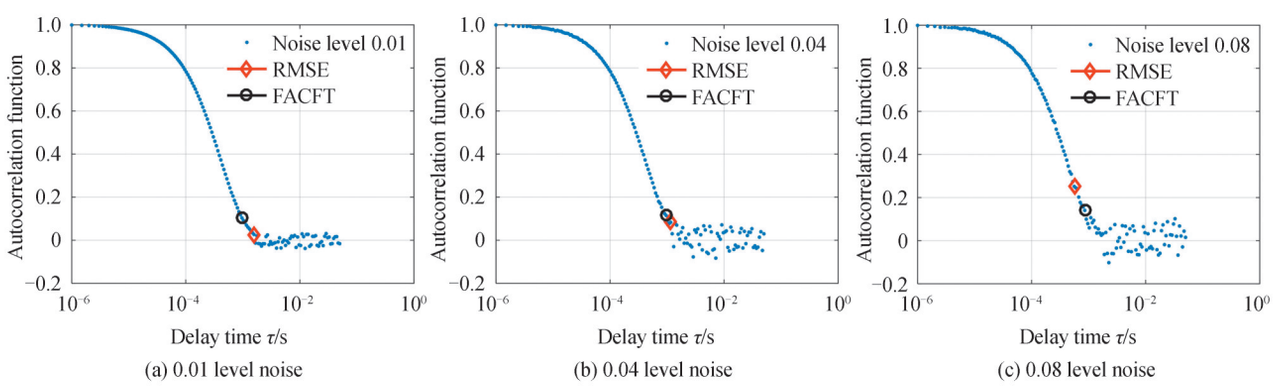

Fig.9 The truncation position of the ACF for the two truncation methods at 0.01 level noise, 0.04 level noise and 0.08 level noise

In the selection of ACF points, since neither the fixed ACF points nor FACFT method can take into account both the measured particle size and ACF noise level, a different approach is required. In Section 3.2, it was observed that the variation of E_{RMS} with the number of ACF points fitted can be divided into two stages: in the first stage E_{RMS} grows smoothly; while in the second stage E_{RMS} grows rapidly. The rapid growth of E_{RMS} indicates that the noise contained in the ACF data increases and the reliability of the ACF data decreases with increasing number of data points. The point of inflection of the E_{RMS} curve marks where the noise contribution from subsequent data points significantly increases the fitting error and produces poorer inversion results. This is an obvious truncation position, which should effectively select the optimal number of ACF points and avoid the influence of noise in the baseline on the inversion results. Fig.4 shows the E_{RMS} variation with the number of ACF data points being fitted for the various samples. It can be seen from Figs.4(a), (b) and (c) that the position of the rapid growth of each E_{RMS} curve is below 0.003 5. With this in mind, we propose a Root-Mean-Square Error Threshold (RMSET) method as the criterion for selecting the optimal number of ACF data points to be fitted. Furthermore, we set 0.003 5 as the E_{RMS} threshold.

It can also be seen from Fig.4 that the number of ACF points corresponding to $E_{\mathrm{RMS}}=0.003\ 5$ increases as the particle size increases. The red ◇ mark in Fig.9 is the selected position using the RMSET method, and the channel number corresponding to this varies with the ACF noise level. The data number of points selected at noise levels of 0.01, 0.04, and 0.08 are 101, 90, and 83 respectively. It is obvious that more ACF points are selected for an ACF with a lower noise level, while fewer ACF points are selected for one with a higher noise level. This shows that RMSET method is adaptable to noise. The RMSET method has obvious advantages

than other methods. It can select the truncation position according to the particle size of the sample and the noise level of the ACF, that is, the larger the particle size to be measured, the more ACF points are used, the smaller the particle size to be measured, the fewer the ACF points, the high-precision ACF takes more ACF points, and the low-precision ACF takes fewer ACF points.

4 Experimental data and analysis

To verify the proposed method, the ACFs for unimodal samples 1 to 5 and bimodal sample 6 were analyzed using the RMSET and FACFT methods and the Tikhonov regularization algorithm for inversion.

Fig.10 shows the truncation positions of the 10 ACFs of sample 3 for the two truncation methods, and Fig.11 shows the corresponding inversion results. Figs.12 and 13 respectively show the fluctuation of the PSD norms and the peak sizes from 60 data sets obtained by the two different truncation methods. The red △ and black ☆ in the figure mark the truncation positions and inversion results of the RMSET and FACFT methods respectively. It can be observed from Fig.10 that the truncation positions of the RMSET method change due to the fluctuation of noise in the ACFs, while the truncation positions of the FACFT method change little. The fluctuations of the norms and peak sizes of the PSDs obtained by the RMSET method are 7.2%, 2.4%, and are smaller than 9.2%, 4.6% obtained by FACFT method, as shown in Fig.12 and Fig.13.

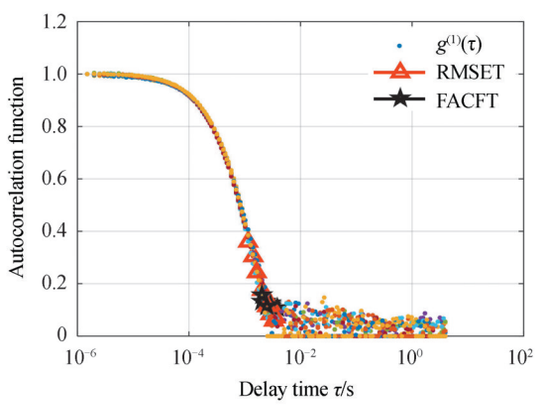

Fig.10 The truncated positions of the electric field ACFs for sample 3 by the two truncation methods

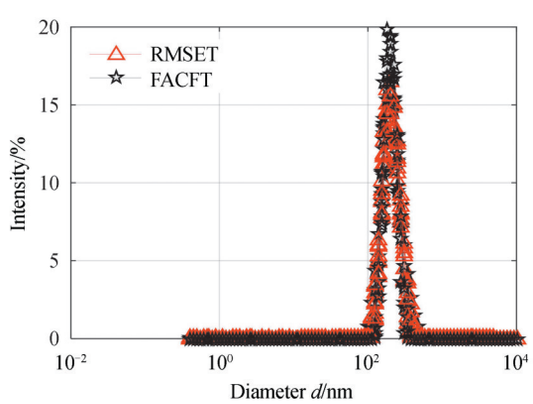

Fig.11 The recovered PSDs of sample 3 by the two truncation methods

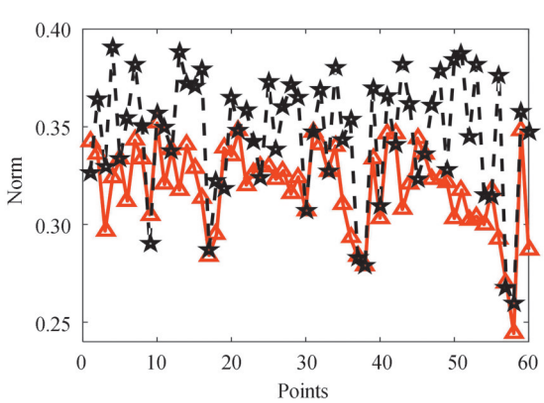

Fig.12 The norms of PSDs of sample 3 from 60 data sets obtained by the two truncation methods

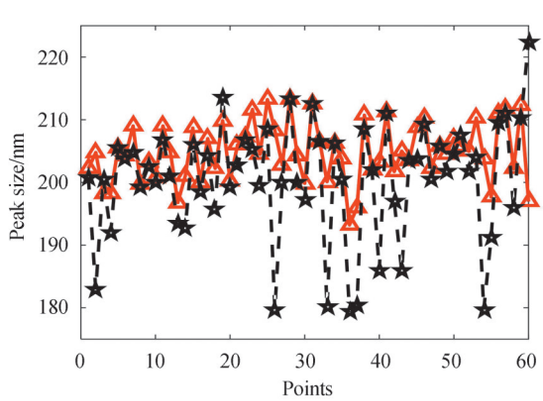

Fig.13 The peak sizes of sample 3 from 60 data sets obtained by the two truncation methods

Table 2 shows the inversion results of 60 data sets of the unimodal samples 1 to 5 obtained by the two truncation methods. It can be seen from Table 2 that for sample 1 and sample 2, the E_{PK} values of the two truncation methods are similar and relatively small, and the stability and repeatability of the results of the RMSET method are slightly higher than that of the FACFT method. For samples 3 to 5, the E_{PK}, V_{RSD} and R_N of the RMSET method are 2.1%, 2.4% and 7.2%, while the FACFT method results are 3.4%, 4.6% and

9.2% repectively. It can be seen from the results that for unimodal samples, the RMSET method has higher accuracy, better stability and repeatability than the FACFT method, and the advantages of the RMSET method is more obvious with increasing particle size.

Table 2 Inversion results for different samples under two truncation methods

No.	E_{RMS}		D_{peak}/nm		E_{PK}/%		PSD width/nm		V_{RSD}/%		R_N/%	
	RMSET	FACFT	RMSET	FACFT	RMSET	FACFT	RMSET	FACFT	RMSET	FACFT	RMSET	FACFT
Sample 1	0.002 6	0.002 5	33.8	33.6	2.8	2.6	25.4	24.8	2.4	2.5	5.6	5.6
Sample 2	0.003 0	0.003 7	63.4	62.9	3.8	3.6	42.7	39.6	1.8	2.5	4.1	5.7
Sample 3	0.003 0	0.005 9	204.5	200.6	2.1	3.4	149.3	125.8	2.4	4.6	7.2	9.2
Sample 4	0.003 1	0.008 9	576.9	526.3	7.1	11.0	514.2	339.7	7.1	13.2	13.8	15.5
Sample 5	0.003 3	0.008 7	1 289.6	1214.9	9.4	13.9	1 376.3	898.8	11.2	17.2	14.4	16.4

For bimodal sample 6, the E_{RMS} of the 6 data sets for different numbers of ACF data points fitted is shown in Fig. 14, and the PSDs recovered by the two truncation methods are shown in Fig. 15. It can be seen from Fig. 14 that the variation of E_{RMS} with the number of ACF data points fitted is consistent with the unimodal samples, and the point of inflection of E_{RMS} is below 0.003 5. Therefore, 0.003 5 is also set as the threshold, which is same as unimodal samples. The inversion results of RMSET and FACFT methods are shown in Table 3.

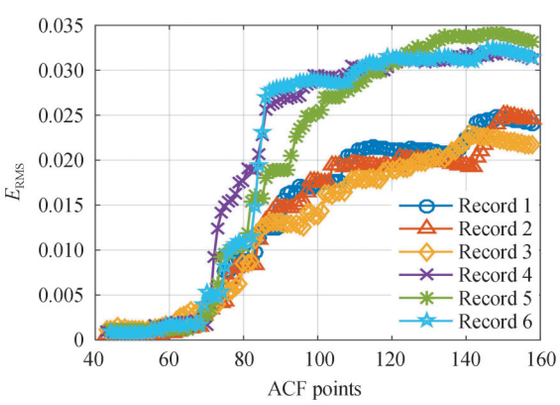

Fig.14 The E_{RMS} of the ACFs at different data points for sample 6

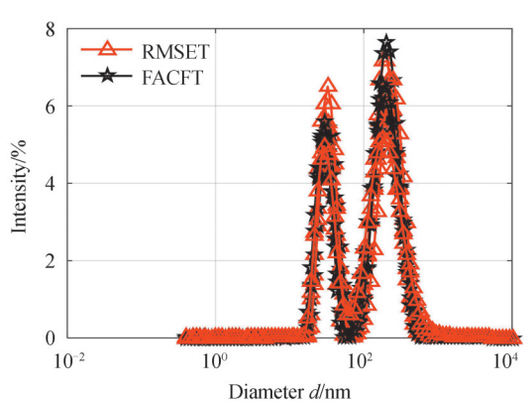

Fig.15 The recovered PSDs of sample 6 by the two truncation methods

In Table 3, D_{peak1} and D_{peak2} are the two peaks of the inversion, E_{PK1} and E_{PK2} are the relative error of the corresponding peak size, V_{RSD1} and V_{RSD2} are the repeatability of the inversion results. According to the experimental data, the E_{PK1} and E_{PK2} values retrieved by the RMSET method are smaller than those of the FACFT method. Also, the values of V_{RSD1} and V_{RSD2} obtained by the RMSET method are smaller than those of the FACFT method. It is notable that the RMSET method also outperforms the FACFT method in terms of inversion results.

Table 3 Inversion results for sample 6 obtained by the two truncation methods

Method	E_{RMS}	D_{peak1}/nm	D_{peak2}/nm	E_{PK1}/%	E_{PK2}/%	V_{RSD1}/%	V_{RSD2}/%	R_N/%
RMSET	0.002 8	31.0	202.2	6.5	3.0	4.2	3.9	6.2
FACFT	0.003 9	29.7	197.8	10.4	4.4	8.9	5.8	9.8

To summarize, the RMSET method used to select the best truncation position for fitting of the ACF can adapt to different samples and has a certain adaptability to different ACF noise levels. Its flexibility is better than the FACFT method. Moreover, this method is not only suitable for unimodal samples but also for multimodal samples.

5 Conclusion

To improve the accuracy and repeatability of the inverted PSDs, we propose a method to obtain the optimal ACF truncation point by using RMSET, that is, truncate the ACF data fitting at the highest correlation channel which has an RMS error smaller than 0.003 5. The advantage of the RMSET method is that it can automatically obtain the best ACF points according to the measured particle size and ACF accuracy, and it is suitable for both unimodal and bimodal samples. For the measured particles of 203 nm, the relative error of the peak size E_{PK} (ie accuracy) obtained by the RMSET method is 2.1%, and the relative standard deviation of particle size V_{RSD} (ie repeatability) is 2.4%, which are both smaller than the E_{PK} value 3.4% and V_{RSD} value 4.6% of the fixed ACF threshold method. The results show that the RMSET method proposed in this paper can effectively improve the accuracy and repeatability of the inversion results, and has an important application value in the field of nanoparticle measurement.

References

[1] PECORA R. Dynamic light scattering: applications of photon correlation spectroscopy[M]. New York: Plenum Press, 1985.

[2] THOMAS J C. Photon correlation spectroscopy: technique and instrumentation[C]. SPIE, 1991.

[3] FRISKEN B J. Revisiting the method of cumulants for the analysis of dynamic light-scattering data[J]. Applied Optics, 2001, 40(24):4087-4091.

[4] LIU Wei, WANG Yajing, SHEN Jin. Optimal fitting Cumulants method for dynamic light scattering[J]. Acta Optica Sinica, 2013, 33(12): 1229001.

[5] MORRISON I D, GRABOWSKI E F, HERB C A. Improved techniques for particle size determination by quasi-elastic light scattering[J]. Langmuir, 1985, 1(4): 496-501.

[6] PROVENCHER S W. A constrained regularization method for inverting data represented by linear algebraic or integral equations[J]. Computer Physics Communications, 1982, 27(3):213-227.

[7] TIKHONOV A N, ARSENIN V Y. Solutions of ill-posed problems[J]. Society for Industrial and Applied Mathematics, 1979, 21(2): 266-267.

[8] GUGLIOTTA L M, STEGMAYER G S, CLEMENTI L A, et al . A neural network model for estimating the particle size distribution of dilute latex from multiangle dynamic light scattering measurements[J]. Particle & Particle Systems Characterization, 2009, 26(1-2): 41-52.

[9] YUAN Xi, LIU Zhenming, WANG Yajing, et al . The non-negative truncated singular value decomposition for adaptive sampling of particle size distribution in dynamic light scattering inversion[J]. Journal of Quantitative Spectroscopy and Radiative Transfer, 2020, 246: 106917.

[10] RUF H. Effects of normalization errors on size distributions obtained from dynamic light scattering data[J]. Biophysical Journal, 1989, 56(1): 67-78.

[11] RUF H, GOULD B J. Use of dynamic light scattering for the determination of size distributions of chylomicrons from human lymph[C]. SPIE, 1997, 2982: 206-213.

[12] RUF H, GOULD B J, HAASE W. The effect of nonrandom errors on the results from regularized inversions of dynamic light scattering data[J]. Langmuir, 1999, 16(2): 471-480.

[13] CLEMENTI L A, VEGA J R, GUGLIOTTA L M, et al . A Bayesian inversion method for estimating the particle size distribution of latexes from multiangle dynamic light scattering measurements[J]. Chemometrics & Intelligent Laboratory Systems, 2011, 107(1):165-173.

[14] BERNE B J, PECORA R. Dynamic light scattering with applications to chemistry, biology, and physics[M]. New York: Dover Publication, 2000.

[15] LIU Wei, WANG Yajing, CHEN Wengang, et al . Evaluation criteria of inversion algorithm for dynamic light scattering [J]. Acta Optica Sinica, 2015, 35(s1): 370-377.

Determination of Optimal Autocorrelation Function Truncation Point for Particle Size Measurement with Dynamic Light Scattering

QI Tiantian[1], LIU Wei[1], THOMAS J C[1,2], JIA Hongyan[1], WEI Qinqin[1], WANG Yajing[1], SHEN Jin[1]

(1 *School of Electrical and Electronic Engineering, Shandong University of Technology, Zibo, Shandong* 255049, *China*)

(2 *Group Scientific Pty Ltd., Grange, South Australia* 5022, *Australia*)

Abstract: Dynamic light scattering technology is a common measurement method that can calculate the particle size distribution of nanoparticles at present. The particle size distribution obtained by the inversion of the autocorrelation function belongs to the problem of solving the first type of Fredholm integral equation, which is a typical ill-posed problem. The data near the baseline of the autocorrelation function has a lot of noise. Therefore, the accuracy and repeatability of the inversion results are affected by the data points of the autocorrelation function, and different data points of the autocorrelation function may lead to different inversion results. To overcome the shortcomings, the characteristics of the root-mean-square error of the fitted correlation function with the number of autocorrelation function points are investigated. The root-mean-square error curve as a function of number of autocorrelation function points can be divided into two stages: in the first stage, the root-mean-square error value of the fitted correlation function grows smoothly with the increase of the number of autocorrelation function points, and in the second stage, as the number of correlation function points increases, the root-mean-square error value of the fitted correlation function grows rapidly. The rapid growth of the root-mean-square error indicates that the noise contained in the autocorrelation function data increases and the reliability of the correlation function data decreases with increasing number of data points. The point of inflection of the root-mean-square error curve marks where the noise contribution from subsequent data points significantly increases the fitting error and produces poorer inversion results. With this in mind, root-mean-square error threshold method as the criterion to truncate the autocorrelation function be proposed. This method adaptively selects the optimal number of autocorrelation function data points by setting the root-mean-square error threshold. It can truncate the autocorrelation function according to the measured particle size and the noise level of the autocorrelation function, and select the optimal autocorrelation function data point. To verify the proposed method, the ACFs for 5 unimodal samples and 1 bimodal sample were analyzed using the root-mean-square error threshold method and the Tikhonov regularization algorithm for inversion. Experimental results show that the particle size results obtained using the root-mean-square error threshold method have higher accuracy and better repeatability than the results obtained by other methods. The root-mean-square error of the fitted correlation function is affected by the noise in the autocorrelation function data, and a larger root-mean-square error value indicates a higher level of noise in the correlation function data, and vice versa. The data near the baseline of the autocorrelation function has a lot of noise, which causes the root-mean-square error value of the fitted correlation function to increase rapidly. Therefore, the root-mean-square error threshold method proposed is essentially realized by using the feature that the root-mean-square value of the fitted correlation function can be used to reflect the noise level of the autocorrelation function data, which can effectively reduce the effect of the noise near the baseline the autocorrelation function on the inversion results.

Key words: Dynamic light scattering; Photon correlation spectroscopy; Optimal data points; Autocorrelation function; Root mean square error; Particle size distribution; Nanoparticle measurement

OCIS Codes: 290.5820; 290.5850; 120.5820